*Exp. Eye Res.* (2002) **75**, 359–363
doi:10.1006/exer.2002.2038, available online at http://www.idealibrary.com on IDEAL®

LETTER TO THE EDITORS

# A Comparison of the Environment of Thiol Groups in Bovine and Human γ Crystallins Using Raman Spectroscopy

γD crystallin is one of the major γ crystallins expressed in the human lens (Siezen et al., 1987). In recent years, several mutations in the γD crystallin gene have been associated with juvenile cataracts (Héon et al., 1999; Stephan et al., 1999; Kmoch et al., 2000). In at least one such inherited form of juvenile cataract, the oxidation of protein thiols and concomitant disulfide-linked aggregation of a mutant of human γD crystallin (the Arg14 to Cys mutant), appears to be the source of opacity (Pande et al., 2000). It is widely accepted that oxidation of protein thiols in the lens is a key mechanism for opacity also in age-onset cataract (Harding and Crabbe, 1984; Harding, 1991). Thus thiol-disulfide exchange reactions are dominant redox reactions in the lens. Since the γ crystallins contain the largest number of cysteine thiols per molecule among the lens crystallins (Wistow et al., 1983; Siezen et al., 1987), the thiol-disulfide redox reactions of these proteins play a significant role in lens transparency and cataract. Therefore, as a first step towards understanding the role of individual protein cysteines in redox reactions in the lens, it is essential to probe the chemical state of thiol groups in these proteins. This can be readily achieved by Raman spectroscopy.

Raman spectroscopy is especially well suited to monitor the redox state of cysteine residues in proteins because the –SH stretching frequency has a signature in an isolated region of the Raman spectrum (approximately 2500–2600 $cm^{-1}$). The frequency of this Raman is a direct measure of the strength of the –S–H bond and, in principle, is an excellent indicator of the molecular interactions involving the –SH group, such as hydrogen bonding. For example, in the case of an –SH···X hydrogen bond, where X is a hydrogen acceptor atom or a group, a strong hydrogen bond between the –SH and X would lead to a weaker –S–H bond and a lower than normal Raman frequency. In general, the stronger the hydrogen bonding of the –SH group the lower the Raman frequency (Li and Thomas, 1991; Raso et al., 2001).

In this report, we compare for the first time, the Raman spectra of human γD (HGD) crystallin with those of bovine γB (BGB) and bovine γD (BGD) crystallins in the spectral regions sensitive to cysteine thiols, aromatic residues and secondary structure of the proteins. The two bovine γ crystallins studied serve as good benchmarks: they have a comparable number of Cys residues to HGD (BGB and BGD have seven and five cysteine residues, respectively, while HGD has six). The cysteine residues are located at positions 15, 18, 22, 32, 41, 78 and 109 (BGB), 18, 32, 41, 78 and 108 (BGD) and 18, 32, 41, 78, 108 and 110 (HGD) in the respective amino acid sequences. The X-ray crystal structures of the two bovine proteins are available at high resolution – 1·2 Å for BGB (Kumaraswamy et al., 1996) and 1·95 Å for BGD (Chirgadze et al., 1996). For HGD, we are currently solving the high-resolution X-ray crystal structure (Basak et al., unpubl. res.). These studies suggest that Cys 108 in BGD and in HGD is spatially equivalent to Cys 109 in BGB. Using the X-ray crystal structures of these proteins and the Raman frequency assignments, our long-term goal is to model the chemical reactivities of all the cysteine residues of the human and bovine γ crystallins. This report constitutes the first step towards this goal.

Spectroscopic studies (Andley et al., 1996; Pande et al., 2000) have already shown that HGD is largely a beta-sheet protein, similar in structure and stability to the other homologous γ crystallins such as BGB and BGD. This is consistent with the Raman spectra shown in Fig. 1. It is apparent from Fig. 1 that all the Raman bands in the 'fingerprint region' (600–1000 $cm^{-1}$) sensitive to aromatic residues, and in the region from 1100 to 1700 $cm^{-1}$ which is sensitive to the secondary structure, are in nearly identical positions for the three proteins. The Amide I bands at 1672 $cm^{-1}$ and Amide III bands at 1238 $cm^{-1}$ are consistent with the predominantly antiparallel beta sheet structure of the γ crystallins (Tu, 1982; Pande et al., 1991). The Raman bands shown are within $\pm 1$ $cm^{-1}$ of those of BGB that we reported earlier (Pande et al., 1991), suggesting that, overall, these proteins have closely similar structures. Several Raman frequencies shown in Fig. 1 are due to aromatic residues – tryptophans at 757, 878, 1546 $cm^{-1}$, tyrosines at 643, 831, 856 and 1209 $cm^{-1}$ and phenylalanine at 1004 and 1031 $cm^{-1}$ (Pande et al., 1991). The ratio of the band intensity (831 $cm^{-1}$/856 $cm^{-1}$) is considered an empirical measure of the degree of H-bonding or the ionization state of the tyrosine –OH groups (Siamwiza et al., 1975). In the γ crystallins this ratio is usually around 1 (Pande et al., 1991), which is found to be the case also for BGB, BGD and HGD

0014-4835/02/$35.00/0

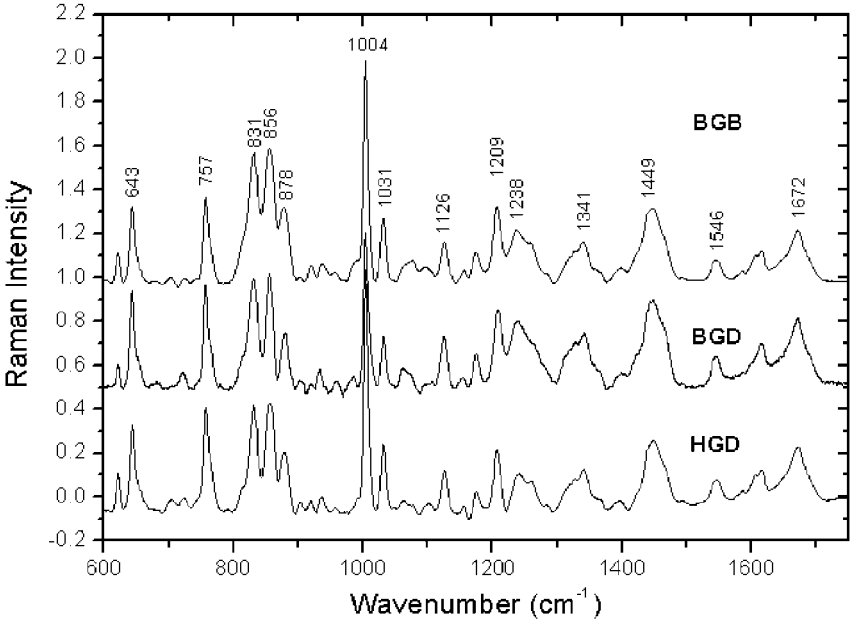


FIG. 1. Comparison of the Raman spectra of BGB, BGD and HGD crystallins in the fingerprint and Amide I regions. The intensity of the Amide I band is lower in all three spectra, compared to our earlier data (Pande et al., 1991). This may be due to the excitation at 785 nm (this work), as opposed to the 488 nm used in our earlier studies in which there was a higher fluorescence background. It may also be due to the difference in the Raman cross section for the Amide I band at the two excitation wavelengths. Protein concentration, 5–10 mM in 0·275 M sodium acetate buffer, pH 5. Spectra were taken at pH 5 to minimize the formation of disulfide-linked aggregates of the protein (Pande et al., 1995) and to maintain them in the reduced form. (Spectra were also taken at pH 7 in 0·1 M sodium phosphate buffer and found to be superimposable with those at pH 5, data not shown.) Samples were contained in stoppered quartz cuvettes and spectra were taken at ambient temperature, with laser excitation at 785 nm from the Argon/Ion (Coherent model Renova 306C, 6 W) laser and titanium/sapphire laser (Coherent model 890 CW, 2·4 W), using a micro-Raman spectrometer, Hololab 5000R made by Kaiser Optical Systems, Inc., Ann Arbor, MI, U.S.A. Power levels at sample typically ranged from 40 to 80 mW. The instrument is built around a Leica DMLP optical microscope. Raman spectra were dispersed at a spectroscopic resolution of 5 cm$^{-1}$ and detected using a thermoelectrically cooled CCD detector at −40°C (1024 × 256 front-illuminated camera from Andor Technology).

(Fig. 1). Small changes in the intensities of these bands could reflect minor variations in the orientations of the corresponding side chains among the three proteins.

Fig. 2 shows the Raman spectra for BGB, BGD and HGD in the region characteristic of the –SH stretch (approximately 2500–2600 cm$^{-1}$). All three spectra are characterized by the –SH Raman doublet typical of the γ crystallins. This doublet is asymmetrical, with a main band around 2580 cm$^{-1}$ and a lower-frequency shoulder near 2560 cm$^{-1}$, as reported earlier by us and by others for several bovine γ crystallins (Pande et al., 1989, 1991; Chen et al., 1991). While the overall –SH band profiles for the three proteins appear to be nearly identical, the area under each profile scales exactly with the number of cysteine residues in the corresponding protein. Thus, the ratio of the –SH bands of BGB/HGD is about 1·20 (i.e. 7/6) and BGB/BGD is 1·4 (i.e. 7/5). This suggests that each Cys residue, on average, makes an equal contribution to the overall –SH band profile for each of these γ crystallins.

A direct comparison of the –SH profiles for the three proteins is justified because (1) there is a high degree of identity (higher than 80 %) in their primary structures; (2) the three proteins show strong similarities also in their secondary and tertiary structures; (3) the cysteine location and distribution is closely similar in these proteins; and (4) as shown above, these cysteines contribute nearly identically to the Raman spectra. These considerations enable us to obtain the Raman difference spectra shown in Fig. 3. In Fig. 3, the upper curve (BGB minus BGD) shows the contribution of Cys 15 and 22 to the –SH band envelope, since these two cysteines are missing in BGD, and Cys 109 in BGB is spatially equivalent to Cys 108 in BGD (as discussed earlier). Similarly, the lower curve (HGD minus BGD) shows the contribution of Cys 110, the additional Cys in the C-terminal domain of HGD, which is missing in BGD. This simple procedure reveals that the sum of the spectral contribution of Cys 15 and 22 includes a small band around 2564 cm$^{-1}$ and a large broad band spanning 2570–2600 cm$^{-1}$. Cys 110 in HGD, however, seems to have a predominant contribution to the 2586 cm$^{-1}$ band with a possible minor contribution near 2560 cm$^{-1}$. We have subsequently produced the Cys to Ser point mutants of all seven cysteines of BGB by site-directed mutagenesis and measured their Raman spectra (Pande et al., 2002). Our preliminary data analysis indicates that there is reasonable agreement between frequency assignments for specific cysteine residues based on our data on the mutants,

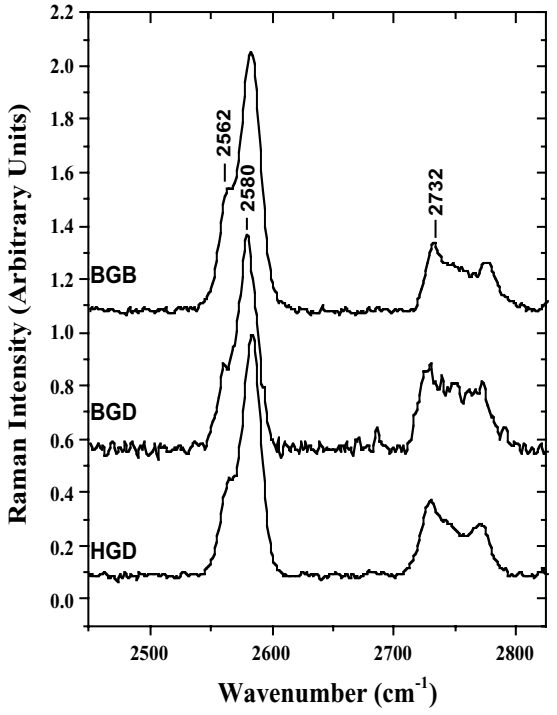


FIG. 2. Raman spectra of BGB, BGD and HGD in the –SH stretching region (2500–2600 $cm^{-1}$). Spectra were accurately aligned using the sharp nitrogen line at 2330·7 $cm^{-1}$ (not shown). The protein skeletal stretching bands around 2700–2800 $cm^{-1}$ were used to normalize the Raman intensity. Experimental conditions are as described in Fig. 1.

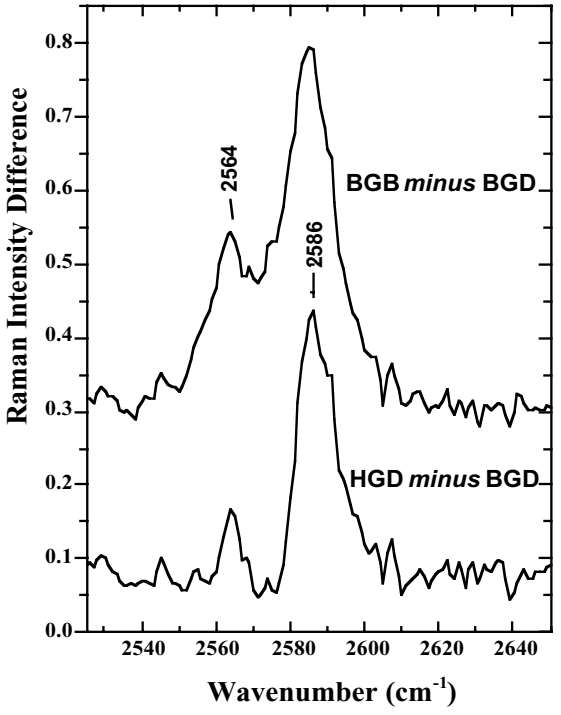


FIG. 3. Raman difference spectra: (BGB minus BGD, upper curve) and (HGD minus BGD, lower curve). The upper difference spectrum shows the sum of the contributions of Cys 15 and 22, i.e. the additional cysteines in BGB not present in BGD. Similarly, the lower difference curve shows the contribution of Cys 110 in HGD.

and the tentative assignments made above based on the native proteins. For example, we find that the sum of the spectral contributions of Cys 15 and 22 obtained from the data on the C15S and C22S mutants (Pande et al., 2002), includes a small band around 2564 $cm^{-1}$ and a large broad band spanning 2570–2600 $cm^{-1}$. This is consistent with the subtracted spectrum shown in Fig. 3 (BGB minus BGD). Similarly, data on the C109S mutant of BGB show that a single band centered around 2586 $cm^{-1}$ can be assigned to Cys 109 in the C-terminal domain, which is analogous to the assignment of a single band to Cys 110 in HGD (Fig. 3, HGD minus BGD).

Using the data in Fig. 3 and the preliminary Raman data on the mutants of BGB mentioned above, we made initial guesses for the peak positions and bandwidths for the appropriate cysteines and obtained curve fits to the data shown in Fig. 2. These fits are shown in Fig. 4. The BGB spectrum was fitted with four Lorentzian curves, while that of BGD and HGD could be fitted better with three Lorentzians in a manner similar to that used for myoglobin (Peterson

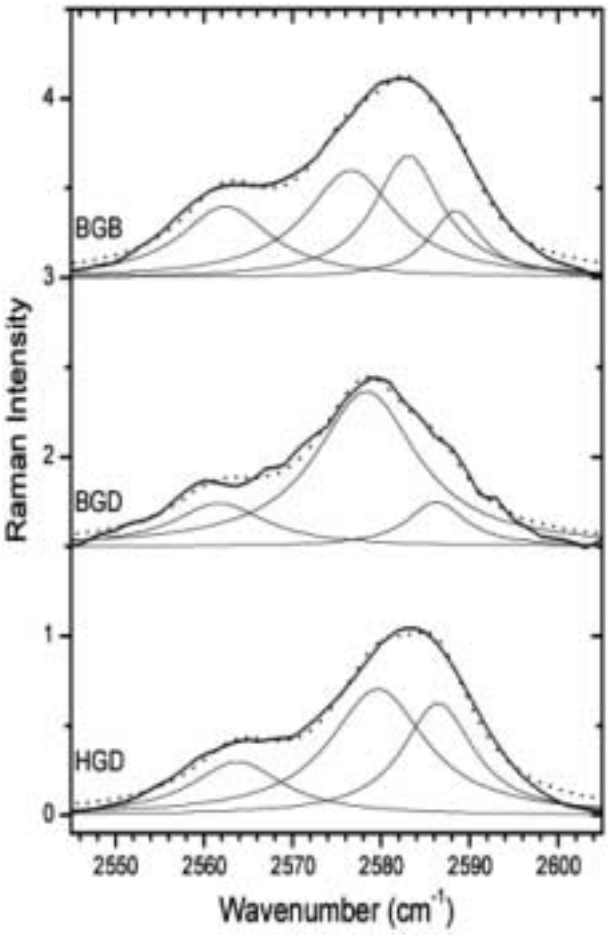


FIG. 4. Curve fitting of the sulfhydryl envelopes of BGB, BGD and HGD shown in Fig. 2. The solid line profile is the measured spectrum and the dotted line profile is the sum of the fitted curves. The individual Lorentzian components obtained by curve-fitting are shown under each sulfhydryl envelope. See text for details.

et al., 1998). The final set of Lorentzian components (Fig. 4) was obtained by varying the amplitudes, widths and center frequencies of each component until they converged to a unique solution. The minimum number of Lorentzian curves was used to obtain a good fit to the data. These fits show that the –SH profile of HGD is closer to that of BGD than to that of BGB. The fits for HGD and BGD differ mainly in the intensity of the Lorentzian component centered around 2587 $cm^{-1}$. In fact, this is clearly observed in the difference spectrum (HGD minus BGD) shown in Fig. 3 and marked as the 2586 $cm^{-1}$ peak. Comparing the Lorentzian components of BGB and BGD in Fig. 4, we notice that the components near 2560 and 2590 $cm^{-1}$ have a higher intensity in BGB. The BGB spectrum is overall, richer in the variety of contributions to the –SH profile than either BGD or HGD. As seen in Fig. 3, this is consistent with the difference-spectrum (BGB minus BGD). Thus the experimental data shown in Figs 2 and 3, while essentially identical, provide alternative means of analyzing the same data.

As already stated, the thiol Raman spectra yield clues to the hydrogen-bonding states of the cysteine residues. The Raman frequency of free cysteine in solution appears at 2580 $cm^{-1}$ (Li and Thomas, 1991) and is indicative of a weak hydrogen bond with water. If one arbitrarily sets a hydrogen bond scale in which –SH frequencies lower than 2580 $cm^{-1}$ represent strong hydrogen bonding and vice-versa, then the difference in the cysteine Raman profiles of HGD and BGD (Fig. 3), suggests that a weakly hydrogen-bonded cysteine (Cys 110) is present in HGD (i.e. –SH stretch near 2586 $cm^{-1}$). In contrast, the difference in the Raman profiles of BGB and BGD is much more complex and suggests a broader spread of hydrogen bonding strengths for Cys 15 + Cys 22 in BGB. These differences in hydrogen bonding patterns between some of the thiols in BGB and HGD may correlate with differences in the reactivities of the –SH groups in these proteins. We have observed earlier that HGD and BGD show similar reactivities in oxidation reactions involving thiol groups (Asherie et al., 1998; Pande et al., 2000), but differ significantly from such reactions in BGB. While such correlations are tentative at this time, our long-term goal is to correlate the reactivities of cysteine residues in the γ crystallins with their sulfhydryl Raman signatures. As a first step towards this goal, we are analysing the Raman data of all the Cys → Ser mutants of BGB as stated above, and have made preliminary assignments to the seven Cys residues of this protein (Pande et al., 2002). These results will be presented elsewhere.

In summary, we have measured for the first time, the Raman spectra of HGD and BGD crystallins and compared the data with those of the well-studied BGB crystallin. The results show that the sulfhydryls of HGD and BGD crystallins are in comparable chemical environments. Using simple subtractions and curve fits to the –SH profiles, we have made initial assignments of the Raman frequencies for some of the cysteine residues. Our analysis shows that the state of sulfhydryls in the γ crystallin family of proteins, even across species, is very similar. The work presented here is an important step towards understanding the sulfhydryl environment in a key γ crystallin, human γD, and will eventually enable us to track changes in sulfhydryl reactivities due to genetic mutations in the protein that lead to cataract (Pande et al., 2000, 2001).

## Acknowledgements

This work was supported by Grants No. EY10535 to J. P. and EY05127 to G. B. We thank Professor Benedek for encouragement and useful discussions. Eugene Hanlon is supported by a grant from the Office of Research and Development, Medical Research Service, Department of Veterans Affairs. Raman measurements were conducted at the MRSEC Shared Facilities at M.I.T., supported by the National Science Foundation under Award Number DMR-9400334 and NSF Laser Facility grant #9708265-CHE. Some earlier work was also done in the NIH supported Laser Biomedical Research Center at M.I.T. (NIH 2P41RR002594-16). Gifts of BGB and HGD clones from Dr Eva Mayr and Dr Nicolette Lubsen, respectively, are gratefully acknowledged, as are consultations with Dr Chandra Pande during the course of this work. We are indebted to Professor J. A. King for providing his laboratory facilities for the expression of the recombinant proteins in *Escherichia coli*, to Mr Olutayo Ogun for protein purification and processing, and to Mr Tim McClure for help with the Raman setup.

JAYANTI PANDE[a]*
EUGENE B. HANLON[b]
AJAY PANDE[a,c]
[a]*Department of Physics, Massachusetts Institute of Technology, Cambridge, MA 02139-4307, U.S.A.*
[b]*Department of Veterans Affairs, Medical Research Service, Bedford, MA 01730, U.S.A.*
[c]*Materials Processing Center, Massachusetts Institute of Technology, Cambridge, MA 02139-4307, U.S.A.*

*Address correspondence to: Jayanti Pande, Department of Physics, 13-2014 M.I.T., 77 Massachusetts Avenue, Cambridge, MA 02139-4307, U.S.A. E-mail: jpande@mit.edu

## References

Andley, U. P., Mathur, S., Griest, T. A. and Petrash, J. M. (1996). Cloning, expression, and chaperone-like activity of human alphaA-crystallin. *J. Biol. Chem.* **271**, 31973–80.

Asherie, N., Pande, J., Lomakin, A., Ogun, O., Hanson, S. R., Smith, J. B. and Benedek, G. B. (1998). Oligomerization and phase separation in globular protein solutions. *Biophys. Chem.* **75**, 213–27.

Chen, W. L., Nie, S. M., Kuck, J. F., Jr. and Yu, N. T. (1991). Near-infrared Fourier transform Raman and conventional Raman studies of calf gamma-crystallins in the lyophilized state and in solution. *Biophys. J.* **60**, 447–55.

Chirgadze, Y. N., Driessen, H. P. C., Wright, G., Slingsby, C., Hay, R. E. and Lindley, P. F. (1996). Structure of the bovine eye lens γD (γIIIb)-crysallin at 1·95 A. *Acta Crystallogr.* **D52**, 712–21.

Harding, J. J. (1991). Chapter 5. In *Cataract: Biochemistry, Epidemiology and Pharmacology*, pp. 195–217. Chapman and Hall: London, U.K.

Harding, J. J. and Crabbe, M. J. C. (1984). The lens: development, proteins, metabolism and cataract. In *The Eye,* 3rd edn. (Davson, H., Ed.), Vol. 1b, pp. 207–492. Academic Press: London, U.K.

Héon, E., Priston, M., Schorderet, D. F., Billingsley, G. D., Girard, P. O., Lubsen, N. and Munier, F. L. (1999). The gamma-crystallins and human cataracts: a puzzle made clearer. *Am. J. Hum. Genet.* **65**, 1261–7.

Kmoch, S., Brynda, J., Asfaw, B., Bezouska, K., Novak, P., Rezacova, P., Ondrova, L., Filipec, M., Sedlacek, J. and Elleder, M. (2000). Link between a novel human gammaD-crystallin allele and a unique cataract phenotype explained by protein crystallography. *Hum. Molec. Genet.* **9**, 1779–86.

Kumaraswamy, V. S., Lindley, P. F., Slingsby, C. and Glover, I. D. (1996). An eye lens protein–water structure: 1·2 Å resolution structure of γB-crystallin at 150 K. *Acta Crystallogr.* **D52**, 611–22.

Li, H. and Thomas, G. J. (1991). Cysteine conformation and sulfhydryl interactions in proteins and viruses. 1. Correlation of the Raman S-H band with hydrogen bonding and intramolecular geometry in model compounds. *J. Am. Chem. Soc.* **113**, 456–62.

Pande, J., Lomakin, A., Fine, B., Ogun, O., Sokolinski, I. and Benedek, G. (1995). Oxidation of gamma II-crystallin solutions yields dimers with a high phase separation temperature. *Proc. Nat. Acad. Sci. U.S.A.* **92**, 1067–71.

Pande, J., McDermott, M. J., Callender, R. H. and Spector, A. (1989). Raman spectroscopic evidence for a disulfide bridge in calf gamma II crystallin. *Arch. Biochem. Biophys.* **269**, 250–5.

Pande, J., McDermott, M. J., Callender, R. H. and Spector, A. (1991). The calf gamma crystallins—a Raman spectroscopic study. *Exp. Eye Res.* **52**, 193–7.

Pande, A., Hanlon, E. and Pande, J. (2002). The sulfhydryls of the gamma crystallins: a vibrational spectroscopic analysis. *Annual Meeting of the Association for Research in Vision and Opthalmology,* May 5–10, 186, Abstr.#4660.

Pande, A., Pande, J., Asherie, N., Lomakin, A., Ogun, O., King, J. and Benedek, G. B. (2001). Crystal cataracts: human genetic cataract caused by protein crystallization. *Proc. Nat. Acad. Sci. U.S.A.* **98**, 6116–20.

Pande, A., Pande, J., Asherie, N., Lomakin, A., Ogun, O., King, J. A., Lubsen, N. H., Walton, D. and Benedek, G. B. (2000). Molecular basis of a progressive juvenile-onset hereditary cataract. *Proc. Nat. Acad. Sci. U.S.A.* **97**, 1993–8.

Peterson, E. S., Friedman, J. M., Chien, E. Y. T. and Sligar, S. G. (1998). Functional implications of the proximal hydrogen-bonding network in myoglobin: a resonance Raman and kinetic study of Leu89, Ser92, His97, and F-helix swap mutants. *Biochemistry* **37**, 12301–19.

Raso, S. W., Clark, P. L., Haase-Pettingell, C., King, J. and Thomas, G. J. Jr. (2001). Distinct cysteine sulfhydryl environments detected by analysis of Raman –SH markers of Cys→Ser mutant proteins. *J. Molec. Biol.* **307**, 899–911.

Siamwiza, M. N., Lord, R. C., Chen, M. C., Takamatsu, T., Harada, I., Matsuura, H. and Shimanouchi, T. (1975). Interpretation of the doublet at 850 and 830 $cm^{-1}$ in the Raman spectra of tyrosyl residues in proteins and certain model compounds. *Biochemistry* **14**, 4870–6.

Siezen, R. J., Thomson, J. A., Kaplan, E. D. and Benedek, G. B. (1987). Human lens gamma-crystallins: isolation, identification, and characterization of the expressed gene products. *Proc. Nat. Acad. Sci. U.S.A.* **84**, 6088–92.

Stephan, D. A., Gillanders, E., Vanderveen, D., Freas-Lutz, D., Wistow, G., Baxevanis, A. D., Robbins, C. M., VanAuken, A., Quesenberry, M. I., Bailey-Wilson, J., Juo, S. H., Trent, J. M., Smith, L. and Brownstein, M. J. (1999). Progressive juvenile-onset punctate cataracts caused by mutation of the gammaD-crystallin gene. *Proc. Nat. Acad. Sci. U.S.A.* **96**, 1008–12.

Tu, A. T. (1982). *Raman Spectroscopy in Biology: Principles and Applications*. Wiley: New York, NY, U.S.A.

Wistow, G., Turnell, B., Summers, L., Slingsby, C., Moss, D., Miller, L., Lindley, P. and Blundell, T. (1983). X-ray analysis of the eye lens protein gamma-II crystallin at 1·9 A resolution. *J. Molec. Biol.* **170**, 175–202.

(*Received 21 May 2002 and accepted in revised form 01 July 2002*)